ACS central science

http://pubs.acs.org/journal/acscii

Research Article

Bone-Specific Enhancement of Antibody Therapy for Breast Cancer Metastasis to Bone

Zeru Tian,[#] Chenfei Yu,[#] Weijie Zhang, Kuan-Lin Wu, Chenhang Wang, Ruchi Gupta, Zhan Xu, Ling Wu, Yuda Chen, Xiang H.-F. Zhang, and Han Xiao*

Cite This: *ACS Cent. Sci.* 2022, 8, 312–321

Read Online

ACCESS | Metrics & More | Article Recommendations | Supporting Information

ABSTRACT: Despite the rapid evolution of therapeutic antibodies, their clinical efficacy in the treatment of bone tumors is hampered due to the inadequate pharmacokinetics and poor bone tissue accessibility of these large macromolecules. Here, we show that engineering therapeutic antibodies with bone-homing peptide sequences dramatically enhances their concentrations in the bone metastatic niche, resulting in significantly reduced survival and progression of breast cancer bone metastases. To enhance the bone tumor-targeting ability of engineered antibodies, we introduced varying numbers of bone-homing peptides into permissive sites of the anti-HER2 antibody, trastuzumab. Compared to the unmodified antibody, the engineered antibodies have similar pharmacokinetics and *in vitro* cytotoxic activity, but exhibit improved bone tumor distribution *in vivo*. Accordingly, in xenograft models of breast cancer metastasis to bone sites, engineered antibodies with enhanced bone specificity exhibit increased inhibition of both initial bone metastases and secondary multiorgan metastases. Furthermore, this engineering strategy is also applied to prepare bone-targeting antibody−drug conjugates with enhanced therapeutic efficacy. These results demonstrate that adding bone-specific targeting to antibody therapy results in robust bone tumor delivery efficacy. This provides a powerful strategy to overcome the poor accessibility of antibodies to the bone tumors and the consequential resistance to the therapy.

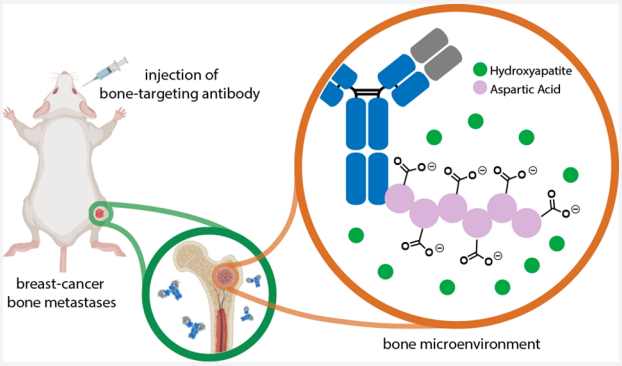

INTRODUCTION

Antibody-based therapies entered the clinic over 30 years ago and have become the mainstream therapeutic option for patients with malignancies,[1,2] infectious diseases,[3,4] and transplant rejection.[5] Compared with traditional chemotherapy, these biotherapeutics preferentially target cells presenting tumor-associated antigens, resulting in improved treatment outcomes and reduced side effects.[6−13] Despite their high affinity for tumor antigens, poor tumor tissue penetration and heterogeneous distribution of therapeutic antibodies in certain tissues, such as brain and bone, have significantly limited their efficacy in treating diseases in these tissues. Failure to deliver efficacious antibody doses throughout the tumor in these tissues leads not only to treatment failure, but also to the development of acquired drug resistance.[14] Furthermore, exposure to subtherapeutic antibody levels has been shown to facilitate tumor cell ability to evade antibody-mediated killing.[15,16] Attempts to ensure effective concentrations of antibodies in the tumor niche usually lead to high concentrations in other tissues, resulting in adverse systemic side effects that may limit or exclude the use of the therapeutic. Thus, strategies to improve tumor penetration and distribution of antibodies in a specific tissue following systemic delivery are crucial for optimizing the clinical potential of these agents.

Despite a 5-year survival rate greater than 90%, 20−40% of breast cancer survivors will eventually experience metastases to distant organs, even decades after the initial diagnosis.[17] Bone is the most frequent site for breast cancer metastasis.[18,19] Dosing the bone microenvironment has proven difficult due to the relatively low density of vascularization and the presence of physical barriers to penetration. Antibody-based therapies face particular distribution difficulties due to their large molecular size. Thus, therapeutic antibodies that exhibit excellent efficacy for the treatment of primary mammary tumors yield only suboptimal responses in patients with bone metastases. For example, the trastuzumab (Herceptin) antibody that successfully targets human epidermal growth factor receptor 2 (HER2) in primary breast tumors has been evaluated as a

Received: August 23, 2021
Published: January 21, 2022

https://doi.org/10.1021/acscentsci.1c01024
ACS Cent. Sci. 2022, 8, 312−321

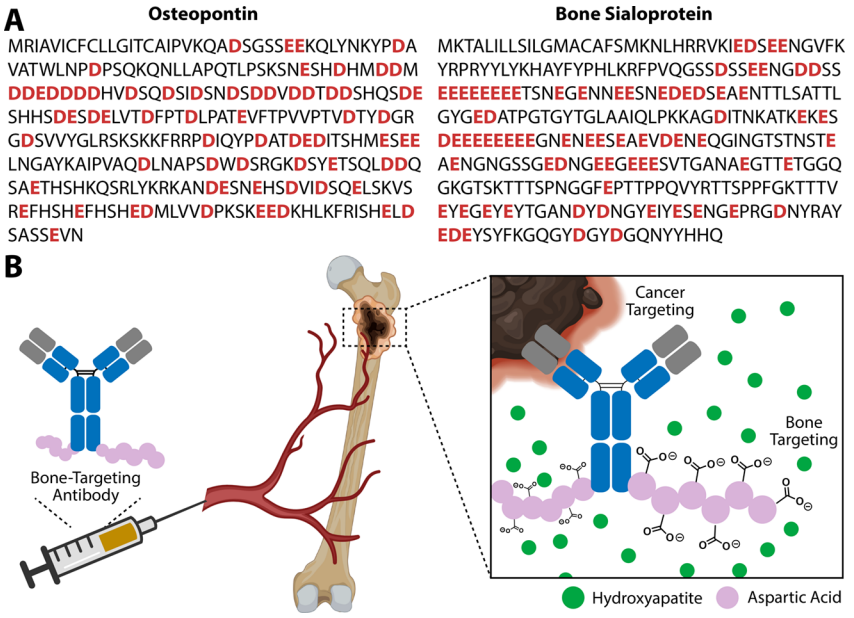

Figure 1. (A) Protein sequences of hydroxyapatite-binding proteins. (B) Therapeutic antibodies can be specifically delivered to the bone by introducing bone-homing peptide sequences that bind to the bone hydroxyapatite matrix.

treatment option for patients with metastatic breast cancer. Although some breast cancer patients benefit from these treatments, a large number of breast cancer patients with bone metastasis experience further tumor progression within one year, and few patients achieve prolonged remission.[20] Thus, the efficacy of therapeutic antibodies appears to be particularly limited in the case of bone metastases.

Bones are primarily composed of hydroxyapatite (HA) crystals, the insoluble salts of calcium and phosphorus. The restricted distribution of HA in hard tissues such as bone makes it an attractive target for selective bone targeting. In fact, Nature has evolved a variety of HA-binding proteins, including sialoprotein and osteopontin, that provide sites for cell anchorage and for modulating the bone mineralization process. Interestingly, sequence analysis reveals that the repeating sequences of acidic amino acids within these proteins represent possible bone-binding motifs (Figure 1A).[21] Polyglutamic acid is known to form a secondary helical structure, while polyaspartic acid is more structurally flexible.[22] To avoid the potential disruption of antibody structure, we will introduce polyaspartic acid into antibodies. Furthermore, short bone-homing peptides consisting of aspartic acid $(Asp)_6$ have been tested for specific delivery of small molecules, microRNAs, and nanoparticles to the bone niche.[23,24] These short peptides have been shown to favor binding to the HA surface with higher levels of crystallinity. This surface is characterized by the presence of bone resorption surfaces and is known as the osteolytic bone metastatic niche.[25,26] Formation of osteolytic bone lesions is driven by paracrine crosstalk among cancer cells, osteoblasts, and osteoclasts.[27,28] Specifically, cancer cells secrete molecules such as parathyroid hormone-related protein (PTHrP) and interleukin 8 that stimulate osteoclast formation directly or indirectly by acting to modulate the expression of osteoblast genes such as receptor activator of nuclear factor-κB ligand (RANKL) and osteoprotegerin (OPG). The consequent increase in bone resorption leads to the release of growth factors (e.g., IGF1) that reciprocally stimulate tumor growth. Thus, selective delivery of therapeutic agents to the bone metastatic niche has the potential to interrupt this vicious osteolytic cycle. Here, we report a general strategy to engineer antibodies with bone-homing peptides for enhanced targeting of bone tumors and demonstrate the engineered antibodies, and antibody-drug conjugates with a moderate bond-targeting capability exhibit optimal efficacy to inhibit breast cancer metastases as well as multiorgan secondary metastases in xenograft models (Figure 1B).

RESULTS

Modifying Trastuzumab with Bone-Homing Peptides. To harness the power of bone-homing peptide for selective delivery of antibodies to bone cancer sites, we first engineered a library of antibodies carrying the bone-homing peptide L-Asp_6 at various sites of the immunoglobulin molecules. Our design principle was to install the bone-homing sequence at sites that would be minimally disruptive to the native IgG structure and function, yet maintain the peptide's high affinity for bone matrix. Based on the crystal structure of an IgG1 monoclonal antibody, we inserted the L-Asp_6 peptide into permissive internal sites in the trastuzumab light chain (LC, A153), heavy chain (CH1, A165), and C-terminus (CT, G449) to yield Tras-LC, Tras-CH1, and Tras-CT, respectively (Figure 2A). These internal sites have been shown to be stable to peptide insertion by screening an antibody peptide-placement library.[29] To modulate the bone tumor-targeting ability of engineered antibodies, we also varied the number of bone-homing peptide sequences per immunoglobulin molecule, generating trastuzumab species with two (Tras-LC/CT, Tras-CH1/CT, and Tras-LC/CH1) and three L-Asp_6 peptide sequences (Tras-LC/CH1/CT). The resulting seven constructs were expressed in ExpiCHO-S cells by transient transfection, followed by purification of immunoglobulins using protein G chromatography and analysis of expressed proteins by SDS-PAGE. To our delight, all these antibody mutants were expressed in good yield (50−100 mg/L). Sodium dodecyl-sulfate polyacrylamide gel electrophoresis (SDS-PAGE) and electrospray ionization mass spectrometry

https://doi.org/10.1021/acscentsci.1c01024
ACS Cent. Sci. 2022, 8, 312−321

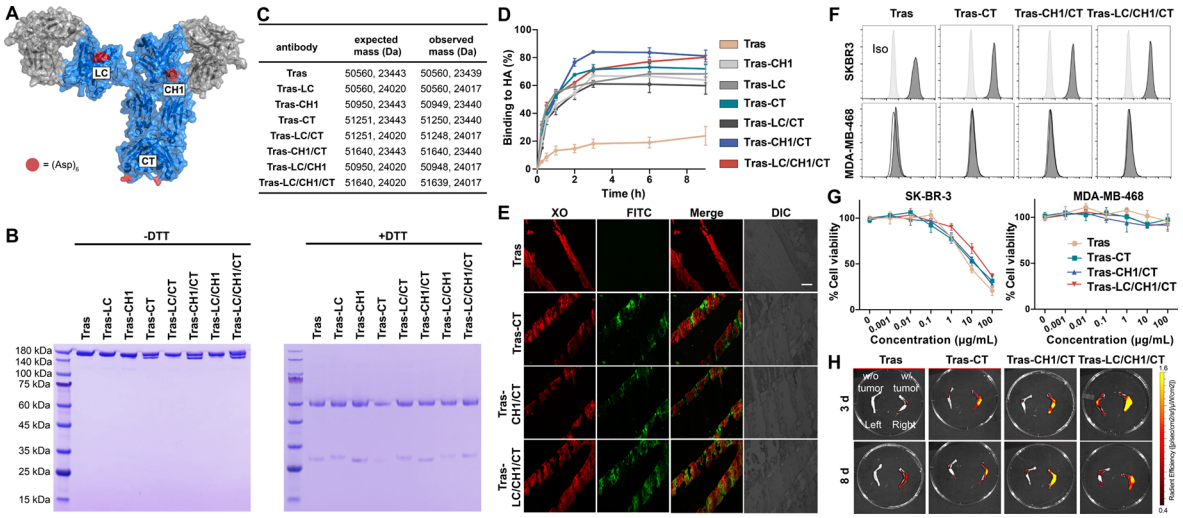

Figure 2. Preparation and characterization of bone-targeting antibodies. (A) We inserted the bone-homing peptide at three locations: light chain (LC), heavy chain (CH1), and c-terminus (CT). (B) SDS-PAGE analysis of bone-targeting antibodies in the absence (left) and presence (right) of the reducing reagents. (C) Mass spectrometry analysis of bone-targeting antibodies. (D) Binding kinetics of Tras, Tras-CH1, Tras-LC, Tras-CT, Tras-LC/CT, Tras-CH1/CT, and Tras-LC/CH1/CT to hydroxyapatite (HA). (E) Differential bone targeting ability of Tras and bone-targeting Tras antibodies. Non-decalcified bone sections from C57/BL6 mice were incubated with 50 μg/mL Tras or bone-targeting Tras antibodies overnight, followed by staining with fluorescein isothiocyanate (FITC)-labeled anti-human IgG and 4 μg/mL xylenol orange (XO, known to label bone), Scale bars, 200 μm. (F) Flow cytometric profiles of Tras, Tras-CT, Tras-CH1/CT, and Tras-LC/CH1/CT binding to SK-BR-3 (HER2+++) and MDA-MB-468 (HER2−) cells. (G) *In vitro* cytotoxicity of Tras, Tras-CT, Tras-CH1/CT, and Tras-LC/CH1/CT against SK-BR-3 and MDA-MB-468 cells. (H) *Ex vivo* fluorescence images of lower limbs of athymic nude mice bearing MDA-MB-361 tumors 72 or 192 h after the retro-orbital injection of Cy7.5-labeled Tras, Tras-CT, Tras-CH1/CT, and Tras-LC/CH1/CT antibodies. Tumor cells were inoculated into the right tibiae of nude mice via para-tibial injection.

(ESI-MS) analysis confirmed the successful insertion of the bone-homing peptides (Figures 2B,C and S1−8). Among the antibody variants, the Tras-LC/CH1 species containing L-Asp_6 peptide sequences in both the light chain and heavy chain exhibited significant aggregation. Thus, this antibody mutant was not studied further.

***In Vitro* Evaluation of Bone-Targeting Antibodies.** With the bone-targeting antibody variants in hand, we initially used a HA binding assay to examine their binding to the mineralized bone. Briefly, bone-targeting antibody species were incubated with HA for varying lengths of time, and unbound antibody remaining in solution was measured using a UV−vis spectrophotometer. As shown in Figure 2D, unmodified Tras exhibited only slight affinity for HA, while L-Asp_6 peptide-modified antibodies bound to HA in a time-dependent manner. As expected, antibodies with multiple L-Asp_6 peptides, namely, Tras-CH1/CT and Tras-LC/CH1/CT, exhibit the highest HA binding capacity, with over 80% of the antibody bound after 9 h of incubation (Table S1). Regarding the three antibody species containing single L-Asp_6 peptides, the C-terminal construct (Tras-CT) exhibits the highest HA binding capacity. Accordingly, fluorescein isothiocyanate (FITC)-labeled Tras, Tras-CT, Tras-CH1/CT, and Tras-LC/CH1/CT were used to stain non-decalcified bone sections from C57BL/6 mice. Sections treated with unmodified Tras exhibited no fluorescence after overnight incubation (Figure 2E). In contrast, we observed FITC signals in all the sections stained with the three L-Asp_6 peptide-containing variants. The FITC signals correlated well with the xylenol orange (XO) signal from the bone (Figures 2E and S9), indicating the enhanced binding of mutant antibodies to the bone.

To demonstrate that insertion of the L-Asp_6 sequence has negligible influence on Tras antibody binding and specificity, FITC-labeled Tras, Tras-CT, Tras-CH1/CT, and Tras-LC/CH1/CT antibodies were tested for binding to HER2-positive and negative cell lines. Flow cytometry reveals that, while none of these antibodies bind to HER2-negative MDA-MB-468 cells, each of the bone-targeting antibodies binds to HER2-expressing SK-BR-3 cells with a K_d similar to that of unmodified Tras (7.09 nM) (Figures 2F and S10−18, and Table S2). The Tras-CT, Tras-LC, Tras-CH1, Tras-CH1/CT, Tras-CH1/CT, and Tras-LC/CH1/CT species have slightly higher K_d values than Tras (14.60 nM, 19.39 nM, 12.99 nM, 19.47 nM, 19.47 nM, and 25.20 nM, respectively) (Figures S10−17), likely due to increased electrostatic repulsion mediated by the inserted negatively charged residues. We next evaluated the *in vitro* cytotoxicity of the bone-targeting antibodies against HER2-positive and negative cell lines. Consistent with the cell binding assay, Tras-CT, Tras-CH1/CT, and Tras-LC/CH1/CT antibodies kill SK-BR-3 cells with an efficiency similar to that of unmodified Tras (EC_{50} values of 5.97 ± 5.64 nM, 13.07 ± 12.09 nM, and 21.10 ± 20.25 nM, respectively) (Figure 2G). In contrast, none of the antibodies exhibit cytotoxicity against HER2-negative MDA-MB-468 cells under the same experimental condition (Figure 2G). These results indicate that introduction of the bone-homing sequence into antibodies can significantly enhance their bone affinity while preserving their antitumor activities *in vitro*. To explore the potential toxicity of Tras-CH1/CT on bone cells, murine preosteoclast cell line RAW264.7 and osteoblast cell line MC3T3-E1 were incubated with various concentrations of Tras or Tras-CH1/CT for 4 days, and cell survival was assessed. As shown in the Figure S19, neither Tras nor Tras-CH1/CT showed significant toxicity. These results indicate that, despite the enhanced binding to the bone, bone-targeting antibodies are unlikely to cause significant toxicity toward bone stromal cells.

https://doi.org/10.1021/acscentsci.1c01024
ACS Cent. Sci. 2022, 8, 312−321

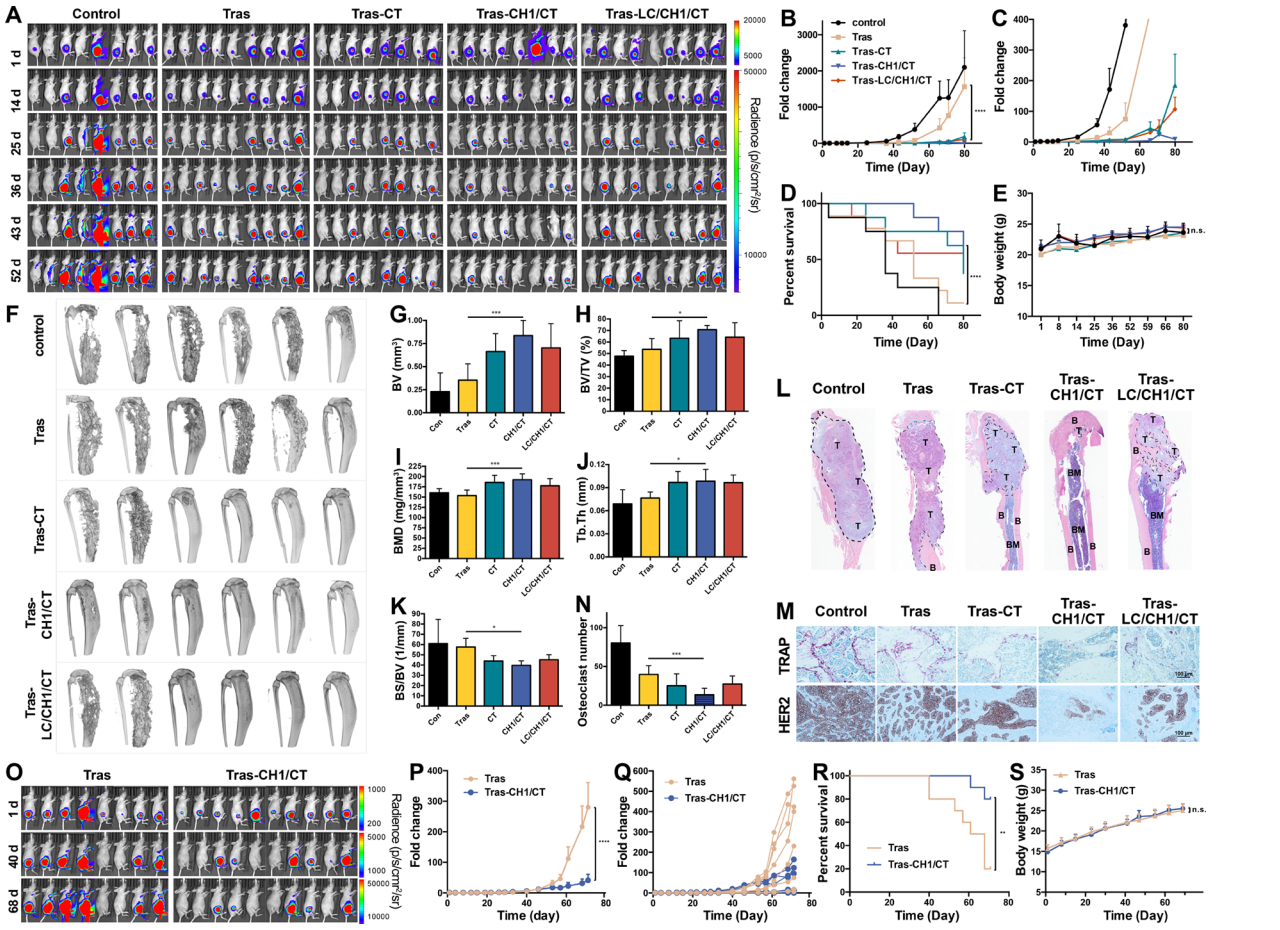

Figure 3. Bone-targeting antibodies inhibit breast cancer bone metastases. (A) MDA-MB-361 cells were para-tibia injected into the right hind limb of nude mice, followed by treatment with PBS, Tras (1 mg/kg retro-orbital venous sinus in sterile PBS twice a week for two months), Tras-CT, Tras-CH1/CT, and Tras-LC/CH1/CT (same as Tras). Tumor burden was monitored by weekly bioluminescence imaging. (B,C) Fold-change in mean luminescent intensity of MDA-MB-361 tumors in mice treated as described in (A). *p* values are based on a two-way ANOVA test. (D) Kaplan−Meier plot of the time-to-euthanasia of mice treated as described in (A). For each individual mouse, the BLI signal in the whole body reached 10^7 photons s^{-1} was considered as the end point. (E) Body weight change of tumor-bearing mice over time. (F) Micro-CT scanning of bones from mice treated with PBS, Tras, Tras-CT, Tras-CH1/CT, and Tras-LC/CH1/CT. (G) Quantitative analysis of bone volume (BV). (H) Quantitative analysis of bone volume/tissue volume ratio (BV/TV). (I) Quantitative analysis of trabecular bone mineral density (BMD). (J) Quantitative analysis of trabecular thickness (Tb.Th). (K) Quantitative analysis of bone surface/bone volume ratio (BS/BV). (L) Representative longitudinal, midsagittal hematoxylin and eosin (H&E)-stained sections of tibia from each group. T: tumor; B: bone; BM: bone marrow. (M) Representative images of HER2 and TRAP staining of bone sections from each group. (N) Osteoclast number per image calculated at the tumor−bone interface in each group (pink cells in (M) were considered as osteoclast positive cells). (O) MDA-MB-361 cells were para-tibia injected into the right hind limb of nude mice, followed by treatment with Tras (10 mg/kg retro-orbital venous sinus in sterile PBS every 2 weeks for two months) and Tras-CH1/CT (same as Tras). Tumor burden was monitored by weekly bioluminescence imaging. (P) Fold-change in mean luminescent intensity of MDA-MB-361 tumors in mice treated as described in (O). (Q) Fold-change in individual luminescent intensity of MDA-MB-361 tumors in mice treated as described in (O). (R) Kaplan−Meier plot of the time-to-euthanasia of mice treated as described in (O). For each individual mouse, the BLI signal in the whole body reached 10^8 photons s^{-1} was considered as the end point. (S) Body weight change of tumor-bearing mice in (O) over time. ****$P < 0.0001$, ***$P < 0.001$, **$P < 0.01$, *$P < 0.05$, and n.s. $P > 0.05$.

***In Vivo* Distribution of Bone-Targeting Antibodies.** The effects of bone-homing peptides on Tras antibody distribution were further investigated in a mouse xenograft model. Using para-tibial injection, 2×10^5 HER2-expressing MDA-MB-361 breast cancer cells labeled with firefly luciferase and red fluorescent protein were first introduced into the right leg of nude mice, followed by administration of sulfo-Cy7.5 labeled Tras, Tras-CT, Tras-CH1/CT, or Tras-LC/CH1/CT via retro-orbital injection. 72 and 192 h after antibody infusion, the major organs were collected and imaged for antibody distribution. The intensity of the interosseous fluorescence signal was stronger in the Tras-CT, Tras-CH1/CT, and Tras-LC/CH1/CT injected animals than that in Tras injected mice (Figures 2H, S20, and S21). As shown in Figure S21A, the quantified *ex vivo* signals from different tissues suggest that a significantly higher signal of bone-targeting antibody could be observed in the skeletal tissues, but not in other tissues (Figure S21B). Furthermore, we performed a histological analysis of collected heart tissues and did not observe obvious pathological variation in cardiac tissues upon different treatments, indicating good biocompatibility of bone-targeting antibodies (Figure S21C). Moreover, larger quantities of bone-targeting antibodies were present in tumor-bearing right leg bones compared to the contralateral bone, likely due to the increased bone resorption in the tumor-bearing bones. Overall, these results indicate that introduction of the L-Asp_6 sequence

https://doi.org/10.1021/acscentsci.1c01024
ACS Cent. Sci. 2022, 8, 312−321

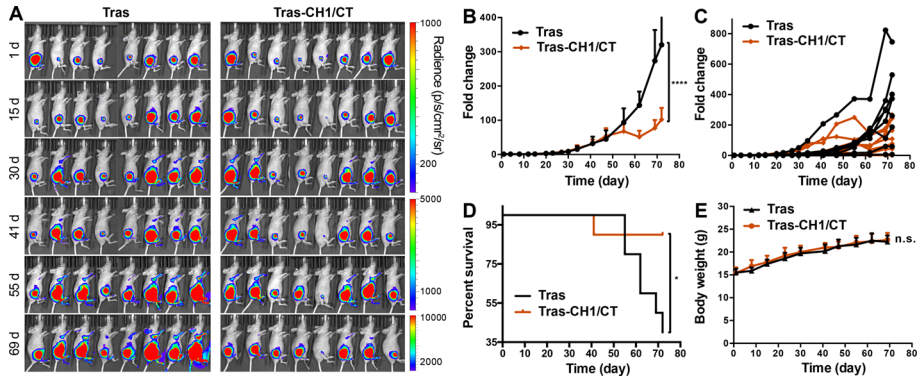

Figure 4. (A) MCF-7 cells were para-tibia injected into the right hind limb of nude mice, followed by treatment with Tras (1 mg/kg retro-orbital venous sinus in sterile PBS twice a week for two months) and Tras-CH1/CT (same as Tras). Tumor burden was monitored by weekly bioluminescence imaging. (B) Fold-change in mean luminescent intensity of MCF-7 tumors in mice treated as described in (A). *p* values are based on a two-way ANOVA test. (C) Fold-change in individual luminescent intensity of MCF-7 tumors in mice treated as described in (A). (D) Kaplan−Meier plot of the time-to-euthanasia of mice treated as described in (A). For each individual mouse, the BLI signal in the whole body reaching 5×10^7 photons s^{-1} was considered the end point. (E) Body weight change of tumor-bearing mice in (A) over time. ****$P < 0.0001$, *$P < 0.05$, and n.s. $P > 0.05$.

enriches therapeutic antibodies in bone tumor sites, which is likely to enhance antitumor activity at the tumor site, while at the same time decreasing systemic toxicity.

***In Vivo* Therapeutic Activity of Bone-Targeting Antibodies against Bone Metastases.** To determine whether bone-targeting antibodies can serve as novel therapeutic entities for the treatment of breast cancer metastasis to bone, we performed *in vivo* antitumor experiments in nude mice bearing MDA-MB-361 bone tumors. We inoculated 2×10^5 MDA-MB-361 breast cancer cells labeled with firefly luciferase and red fluorescent protein into the right leg of nude mice via para-tibial injection. One week after injection, wild-type Tras and bone-targeting Tras antibodies were administered by retro-orbital injection. As shown in Figure 3A, mice receiving 1 mg/kg of unmodified Tras did not respond well to this treatment. Despite an initial inhibitory effect during the first 2 weeks of treatment, unmodified Tras failed to control long-term tumor growth, prolonging the median survival of subjects by only 9.7 days (Figure 3B and C). In contrast, the bone tumor growth was significantly inhibited upon the treatment of bone targeting antibodies. Tras-CT-, Tras-CH1/CT-, and Tras-LC/CH1/CT-treated groups exhibited pronounced delays in tumor growth of 27.5, 35.8, and 18.9 days, respectively (Figure 3B and C). Figures 3A−C, S22, and S23, and Table S3 show the bioluminescent (BLI) signals for each treatment group from day 1 to day 80. In the PBS-treated control group, there was a progressive increase in the BLI signal over time. The BLI signals from day 1 to 80 demonstrate that bone-targeting Tras antibody-treated groups experienced significant delays in tumor growth compared to the Tras-treated group (Figure 3B and C). Mice treated with Tras-CH1/CT exhibited the smallest increases in tumor size (Tras-CH1/CT vs Tras: 9.3 ± 4.2 vs 1562.7 ± 801.6, $p < 0.0001$). Furthermore, the Tras-CH1/CT-treated mice experienced a 62.5% rate of survival at the end point of *in vivo* experiment, compared to 11.1% survival rate in Tras-treated mice (Figure 3D). Thus, treatment with Tras-CH1/CT results in more effective inhibition of bone metastasis progression than wild-type Tras. In addition, treatment with bone-targeting antibodies was well tolerated, as no overt signs of toxicity were observed in any of the treatment groups. For instance, no difference in body weight was observed across the various treatment groups (Figure 3E).

At the end of the experiment (day 81), tibiae (from tumor-bearing legs) were harvested and scanned by microcomputed tomography (micro-CT). Tibias from PBS- and Tras-treated groups showed extensive osteolytic bone destruction, compared to tumor-free tibias (Sham group) (Figures 3F and S24−26). To our delight, tibias from Tras-CH1/CT-treated mice exhibited greater bone volume (BV, Figure 3G), greater bone volume/tissue volume ratio (BV/TV, Figure 3H), greater bone mineral density (BMD, Figure 3I), and thicker trabecular bone (Tb.Th, Figure 3J), but smaller bone surface/bone volume ratio (BS/BV, Figure 3K and Table S4) than those from PBS- and Tras-treated groups. In addition, those parameters showed no significant difference between tibias from Tras-CH1/CT and Sham groups, suggesting Tras-CH1/CT treatment significantly inhibited the bone destruction during metastatic tumor growth (Figure S24). Histological analysis further supports the massive invasion of tumor cells into the bone matrix and the adjacent tissue in the PBS- and Tras-treated groups, while treatment with bone targeting antibodies significantly reduced the tumor burden and preserved normal bone morphology (Figures 3L and S24G). Bone samples from the various treatment groups were also analyzed for bone-resorbing TRAP (tartrate resistant acid phosphatase) positive multinucleated osteoclasts (shown as pink cells) and HER-expressing cancer cells (Figures 3M,N and S27−29). Compared to Tras treatment, Tras-CH1/CT treatment significantly reduces the numbers of both osteoclasts and HER2-positive cells in bone tissues, once again supporting the enhanced ability of bone targeting antibodies to inhibit metastasis progression (Figure 3M and N). Given that tumor-induced hypercalcemia and TRACP 5b protein are the indicators of osteolytic bone destruction, the effects of bone-targeting antibody treatment were evaluated. Consistent with the microCT and histological analysis, Tras-CH1/CT treatment showed the lowest level of bone destruction as evaluated by hypercalcemia and TRACP 5b protein levels in the serum (Figure S30). To evaluate the stability of the bone-targeting antibodies *in vitro*, Tras and Tras-CH1/CT (1 mg/mL, 100 μL) were incubated in PBS at 4 °C for 3 months. SDS-PAGE and ESI-MS analysis revealed that no significant

https://doi.org/10.1021/acscentsci.1c01024
ACS Cent. Sci. 2022, 8, 312−321

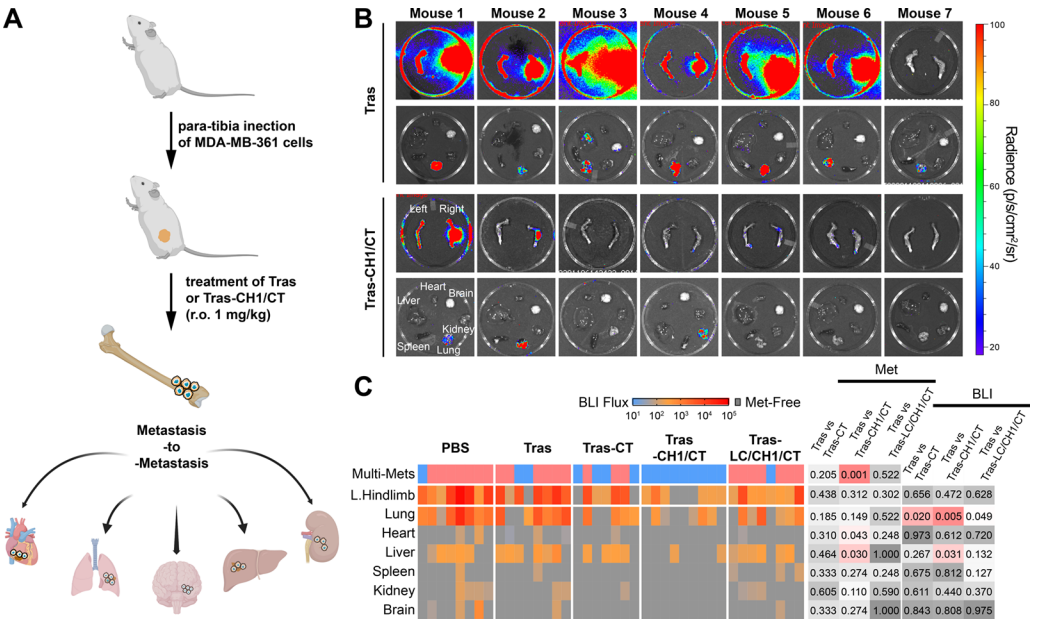

Figure 5. (A) Bone lesions more readily give rise to secondary metastases to multiple organs. (B) Secondary metastases observed in various organs in mice treated with Tras or Tras-CH1/CT. (C) Heat map of *ex vivo* BLI intensity and status of metastatic involvement in tissues from mice treated with PBS, Tras, Tras-CT, Tras-CH1/CT, and Tras-LC/CH1/CT. Each column represents an individual animal, and each row represents a type of tissue. The presence of the metastasis was defined as the presence of BLI signal above 18 counts/pixel under 120 s exposure time. Multisite metastases were defined as the metastatic involvement of at least three tissues. *p*-Values were determined by Fisher's exact test on the frequency of metastatic involvement while by the Mann−Whitney test of the metastatic burden.

degradation or aggregation of bone-targeting antibodies was observed (Figure S31). In the meantime, the serum levels of both Tras and Tras-CH1/CT showed a similar pharmacokinetics *in vivo* (Figure S32), suggesting that the addition of bone-homing peptides does not alter the stability of antibodies.

Next, we evaluated the benefits of bone-targeting antibodies for bone metastasis at a higher dose. Nude mice with MDA-MB-361 bone metastases were treated with Tras or Tras-CH1/CT at 10 mg/kg every 2 weeks. Notably, Tras-CH1/CT treatment results in statistically significant growth inhibition and prolonged overall survival, compared to treatment with 10 mg/kg of Tras (Figures 3O−R, S33, and S34). Furthermore, no weight loss was observed with a high dose of bone-targeting antibodies (Figure 3S).

We also evaluated the enhanced therapeutic efficacy of bone-targeting antibodies with a secondary bone metastasis model using MCF-7 breast cancer cells. Consistent with MDA-MB-361 models, a significant reduction in metastatic burden and increase of mouse survival were observed in the Tras-CH1/CT-treated group, compared to the Tras-treated group (Figures 4A−D and S35). Tras-CH1/CT treatment did not alter additional weight change in animals (Figure 4E).

To examine the efficacy of Tras-CH1/CT in treating primary tumors, we injected MDA-MB-361 cells (1×10^6) in mammary fat pads followed by the treatment of PBS, Tras (1 mg/kg), or Tras-CH1/CT (1 mg/kg). As shown in Figure S36A−C, while both Tras and Tras-CH1/CT treatments significantly decreased the tumor growth in the mammary fat pads, there were no statistical differences in tumor size between two treatments (Figure S36C). Taken together, these data suggest that the introduction of bone-homing peptides into antibodies can significantly inhibit breast cancer bone metastases without compromising its antitumor activity in primary tumors.

Immunogenicity Assessment of Bone-Targeting Antibodies. To understand if the treatment of bone-targeting antibodies causes specific immune responses, we treated immunocompetent C57BL/6J mice with PBS, Tras, or Tras-CH1/CT twice a week for 2 weeks. As shown in Figure S37A, the immunoprofiling determined by flow cytometry suggests that mice treated with either Tras or Tras-CH1/CT had similar immune composition except $CD4^+$ T cells. Furthermore, the IFNγ staining of $CD4^+$ T cells had no significant difference in Tras- and Tras-CH1/CT-treated mice, indicating that Tras-CH1/CT does not significantly alter the functional activity of $CD4^+$ T cells (Figure S37B). Furthermore, there were no significant differences in serum levels of INFγ, IL-2, and IL-4 levels between treatments with wild-type antibodies or bone-targeting antibodies (Figure S37C−E). The above results indicated that adding L-Asp_6 to antibodies does not cause any obvious extra immune response. Furthermore, the *in vivo* immune response to the bone-targeting antibodies can also be tested by an immunogenicity test based on an anti-trastuzumab antibody ELISA-based assay as previously reported.[30,31] To our delight, similar anti-trastuzumab antibody levels were observed in animals treated with Tras (5 mg/kg) or Tras-CH1/CT (5 mg/kg), which suggests that the addition of bone targeting peptides will not alter the immunogenicity of antibodies (Figure S38).

Bone-Targeting Antibodies Prevent Secondary Metastases from Bone Lesions. We have recently reported that established bone lesions may seed multiorgan metastases in the late stage of disease, which dramatically reduces the survival rate of breast cancer patients with bone metastasis in the clinic (Figure 5A).[32−34] Hence, it is imperative for us to evaluate whether bone-targeting antibodies can also impede these secondary metastases derived from bone lesions. Toward this end, 2×10^5 luciferase-labeled MDA-MB-361 cells were introduced into the right hind limbs of nude mice via para-

https://doi.org/10.1021/acscentsci.1c01024
ACS Cent. Sci. 2022, 8, 312−321

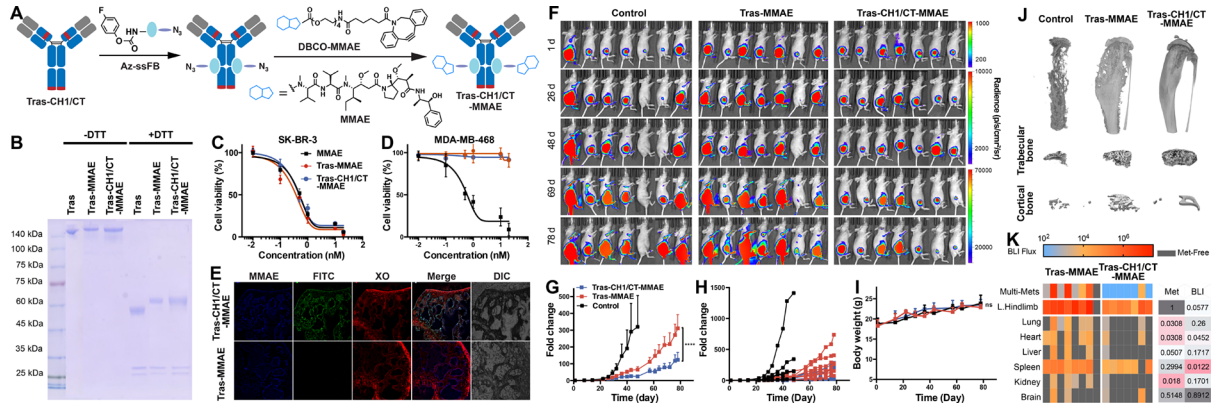

Figure 6. (A) Preparation of bone-targeting antibody-drug conjugates. Tras antibody was first modified with the bone-homing peptide at the heavy chain (CH1) and c-terminus (CT), followed by the modification of MMAE using pClick antibody conjugation technology. (B) SDS-PAGE analysis of Tras-MMAE and Tras-CH1/CT-MMAE under nonreducing (left) and reducing (right) conditions. (C,D) *In vitro* cytotoxicity of MMAE, Tras-MMAE, and Tras-CH1/CT-MMAE, against SK-BR-3 and MDA-MB-468 cancer cells. (E) Differential bone targeting ability of Tras-MMAE and Tras-CH1/CT-MMAE. Non-decalcified bone sections from C57/BL6 mice were incubated with 50 μg/mL Tras-MMAE and Tras-CH1/CT-MMAE overnight, followed by staining with fluorescein isothiocyanate (FITC)-labeled anti-human IgG and 4 μg/mL xylenol orange (XO, known to label bone). (F) MDA-MB-361 cells were para-tibia injected into the right hind limb of nude mice, followed by treatment with Tras-MMAE (0.5 mg/kg retro-orbital venous sinus in sterile PBS every week for two months) and Tras-CH1/CT-MMAE (same as Tras). Tumor burden was monitored by weekly bioluminescence imaging. (G) Fold-change in mean luminescent intensity of MDA-MB-361 tumors in mice treated as described in (F). (H) Fold-change in individual luminescent intensity of MDA-MB-361 tumors in mice treated as described in (F). (I) Body weight change of tumor-bearing mice in (F) over time. (J) Micro-CT scanning of bones from mice treated with Tras-MMAE and Tras-CH1/CT-MMAE after tumor implantation. (K) Heat map of *ex vivo* BLI intensity and status of metastatic involvement in tissues from mice treated with Tras-MMAE and Tras-CH1/CT-MMAE. Each column represents an individual animal, and each row represents a type of tissue. The presence of the metastasis was defined as the presence of BLI signal above 18 counts/pixel under 120 s exposure time. Multisite metastases were defined as the metastatic involvement of at least three tissues. *p* Values were determined by Fisher's exact test on the frequency of metastatic involvement and by the Mann–Whitney test of on the metastatic burden. ****$P < 0.0001$ and n.s. $P > 0.05$.

tibial injection, followed by treatment with unmodified Tras and bone-targeting Tras antibodies. In this model, highly localized tumors were developed in tibiae at an early stage, but as the bone lesion progresses, metastases marked by bioluminescence signals began to appear in other organs, including other bones, lungs, heart, liver, spleen, kidney, and brain. At the end point, these organs were dissected for assessment of metastasis. As shown in Figures 5B,C and S39, treatment with Tras-CH1/CT significantly reduces the frequency of secondary metastasis to the contralateral hind limb (left hindlimb bone), heart, and liver. The metastatic burden of secondary metastases from primary bone lesions was also reduced in mice treated with bone-targeting antibodies, especially with Tras-CH1/CT treatment. Compared to unmodified Tras, Tras-CH1/CT also significantly reduced the metastatic burden in the lung and liver (Figures 5C and S39). Taken together, these data support the enhanced therapeutic efficacy of bone-targeting antibodies against both primary bone metastases and secondary metastases from the bone metastases.

Modification of Antibody-Drug Conjugates with the Bone-Homing Peptide Exhibit Enhanced Therapeutic Efficacy *in Vivo*. Antibody-drug conjugates (ADCs) that combine the antibody's tumor specificity with the high toxicity of chemotherapy drugs are emerging as an important class of anticancer drugs for breast cancer patients, especially ones with advanced breast cancer.[35,36] Following the first FDA approval of trastuzumab emtansine (T-DM1) for HER2-positive breast cancer, trastuzumab deruxtecan has been recently approved for the treatment of adults with unresectable or metastatic HER2-positive breast cancers.[37,38] To test if bone-targeting ADCs can further improve their efficacy in treating bone metastases, we first used pClick conjugation technology to site-specifically couple the monomethyl auristatin E (MMAE) to both wild-type antibody Tras and the bone-targeting antibody Tras-CH1/CT (Figure 6A).[39,40] The successful conjugation was demonstrated by SDS–PAGE and ESI-MS (Figures 6B, S40, and S41). To ensure that conjugation of toxin did not alter the antigen targeting ability and specificity, the *in vitro* binding assays were performed using HER2-positive and -negative cells (Figure S42). Tras-CH1/CT-MMAE showed a high binding affinity to HER2-positive SK-BR-3 cells, but not HER2-negative MDA-MB-468 cells. Next, we evaluated the *in vitro* cytotoxicity of these ADCs in SK-BR-3 and MDA-MB-468 breast cancer cell lines (Figure 6C and D). Both Tras-MMAE and Tras-CH1/CT-MMAE exhibited high potency only in the SK-BR-3 (EC50:0.18 ± 0.82 nM and 0.49 ± 0.30 nM, respectively), with no significant toxicity was observed in the MDA-MB-468 cells. To test the bone targeting ability of Tras-CH1/CT-MMAE *in vitro*, we incubated either Tras-CH1/CT-MMAE or Tras-MMAE with nondecalcified bone sections. As expected, only the signal of Tras-CH1/CT-MMAE correlated well with the XO signal, confirming its bone-targeting ability (Figure 6E).

Next, we examined the therapeutic efficacy of bone-targeting ADCs in the xenograft model of bone metastasis. Weekly administration of the Tras-CH1/CT-MMAE led to a significant inhibition of metastatic growth in bone, compared to unmodified Tras-MMAE (Figures 6F–H, S43, and S44). Furthermore, the bone-targeting ADC showed no apparent toxicity, as indicated by continuous increase of body weight across the different groups during treatment (Figure 6I). The micro-CT analysis revealed extensive osteolytic bone destructions in both the PBS- and Tras-MMAE-treated group, but not in Tras-CH1/CT-MMAE-treated group (Figures 6J and S45). Compared to mice in the PBS- and Tras-MMAE-treated

https://doi.org/10.1021/acscentsci.1c01024
ACS Cent. Sci. 2022, 8, 312–321

groups, Tras-CH1/CT-MMAE-treated mice exhibited higher bone volume/tissue volume ratio (BV/TV, Figure S46A) and thicker trabecular bone (Tb.Th, Figure S46B). Histology also confirms the reduction of intratibia tumor burden in Tras-CH1/CT-MMAE mice (Figure S47). Consistently, bone-targeting ADC also significantly reduced the frequency and size of secondary metastases derived from bone lesions (Figures 6K and S48).

DISCUSSION

Antibody therapy has evolved to focus on finding new biomarkers and on functionalizing antibodies with new payloads. We now demonstrate that adding the bone homing capability to therapeutic antibodies can improve their tumor-specific distribution, thereby enhancing therapeutic efficacy. Failure to achieve an efficacious dose in the tissue of interest is a major challenge for many antibody-based therapeutics. Incomplete access of therapeutics to all cells in tumor tissues can lead to treatment failure and the development of acquired drug resistance. As an example, therapeutic antibodies that exhibit excellent efficacy in the treatment of primary tumors often yield suboptimal responses against bone or brain metastases that offer limited access to macromolecules. Furthermore, antibody-based therapeutics are often associated with unacceptable "on-target" toxicity in cases in which specific antigens are also present in healthy tissues.[41] For example, the use of trastuzumab for breast cancers that overexpress HER2 is associated with rare but fatal lung toxicity, referred to as interstitial lung disease. Therefore, improvements in selective delivery of antibodies to tumors in specific microenvironments provide a promising avenue for advancing new anticancer therapies toward clinical translation.

Antibody-based trastuzumab (Herceptin) and pertuzumab (Perjeta) therapies are established as the standard of care for HER2+ adjuvant and metastatic breast cancer.[42,43] Although many HER2+ bone metastatic breast cancer patients benefit from these treatments, few experience prolonged remission.[16,44−46] Of patients with HER2-positive bone metastases, only 17% achieved a complete response and none achieved a durable complete response. By comparison, 40% and 30% of patients with liver metastases achieved complete responses and durable complete responses, respectively. As another example, a recent phase III clinical trial revealed that immune checkpoint blockade antibodies do not benefit patients with bone metastases.[45] Thus, strategies for improving the outcomes of breast cancer patients with bone metastases are highly desired. In our previous work, we developed a bone-targeting antibody by site-specific conjugation of trastuzumab with a bisphosphonate, alendronate, using the pClick technology.[40,46] The resulting bone-targeting antibody was demonstrated to be effective in treating breast cancer bone metastasis in preclinical models.[46] Alendronate has a strong affinity for calcium phosphate surfaces. However, it is important to test the antitumor activities of antibodies with various bone-targeting abilities, as excessive affinity to bones may lead to reduced accessibility to entire metastatic lesions.

In this study, we demonstrated that adding bone-homing peptides to therapeutic antibodies leads to increased antibody distributions in the bone metastases. Using xenograft models of bone metastasis, we find that unmodified trastuzumab has poor bone tissue penetration and distribution, thus reducing access of the antibody to its target and limiting its efficacy against cancer cells in the bone microenvironment. Compared with the unmodified antibody, trastuzumab modified with bone-homing peptide sequences (L-Asp_6) exhibited enhanced targeting to sites of bone metastasis. This approach yields a targeted therapy against the growth of primary bone metastases as well as the further dissemination from established bone lesions. Most importantly, we demonstrate that the modified antibody and antibody-drug conjugate with moderate bone-binding capability have optimal efficacy *in vivo*. In contrast, an antibody with higher bone-binding capability has suboptimal activity against bone metastases. This may be due to the slow release of the latter entity from the bone matrix or to increased electrostatic repulsion resulting from the increased number of peptides with negative charges. The addition of bone specificity to antibody therapy enables the specific delivery of these agents to the bone. This study establishes a new strategy for transitioning antibody-based therapies from antigen-specific to both antigen- and tissue-specific. This approach not only enhances the therapeutic efficacy in treating bone tumors, but may also reduce adverse side effects associated with the systemic distribution of the drug, thus providing a promising new avenue for advancing antibody therapy toward clinical translation.

ASSOCIATED CONTENT

Supporting Information

The Supporting Information is available free of charge at https://pubs.acs.org/doi/10.1021/acscentsci.1c01024.

Materials methods; DNA oligomers; expression and purification of antibody mutants; protein sequences of antibodies; supplementary figures (Figure S1−S48); supplementary tables (Table S1−S4) (PDF)

AUTHOR INFORMATION

Corresponding Author

Han Xiao − *Department of Chemistry, Department of Biosciences, and Department of Bioengineering, Rice University, Houston, Texas 77005, United States;* orcid.org/0000-0002-4311-971X; Email: han.xiao@rice.edu

Authors

Zeru Tian − *Department of Chemistry, Rice University, Houston, Texas 77005, United States*

Chenfei Yu − *Department of Chemistry, Rice University, Houston, Texas 77005, United States*

Weijie Zhang − *Lester and Sue Smith Breast Center, Baylor College of Medicine, Houston, Texas 77030, United States*

Kuan-Lin Wu − *Department of Chemistry, Rice University, Houston, Texas 77005, United States*

Chenhang Wang − *Department of Chemistry, Rice University, Houston, Texas 77005, United States*

Ruchi Gupta − *Department of Chemistry, Rice University, Houston, Texas 77005, United States*

Zhan Xu − *Lester and Sue Smith Breast Center, Baylor College of Medicine, Houston, Texas 77030, United States*

Ling Wu − *Lester and Sue Smith Breast Center, Baylor College of Medicine, Houston, Texas 77030, United States*

Yuda Chen − *Department of Chemistry, Rice University, Houston, Texas 77005, United States*

Xiang H.-F. Zhang − *Lester and Sue Smith Breast Center, Baylor College of Medicine, Houston, Texas 77030, United States*

https://doi.org/10.1021/acscentsci.1c01024
ACS Cent. Sci. 2022, 8, 312−321

Complete contact information is available at:
https://pubs.acs.org/10.1021/acscentsci.1c01024

Author Contributions

[#]Z.T., C.Y., X.H.-F.Z., and H.X. developed the hypothesis, designed experiments, analyzed the data, and wrote the manuscript. Z.T., C.Y., W.Z, K.-L.W., R.G., Z.X., and L.W. performed experiments. W.Z., Y.C., X.H.-F.Z., and H.X. contributed to experimental design, generation of the reagents, and manuscript editing. X.H.-F.Z. and H.X. conceived and supervised the project. Z.T. and C.Y. contributed equally.

Notes

The authors declare no competing financial interest.

■ ACKNOWLEDGMENTS

We thank Dr. Xiao and Zhang Laboratory members for insightful comments. This work was supported by the Cancer Prevention Research Institute of Texas (CPRIT RR170014 to H.X.), NIH (R35-GM133706, R21-CA255894, and R01-AI165079 to H.X., CA183878 and CA221946 to X.H.-F.Z.), the Robert A. Welch Foundation (C-1970 to H.X.), US Department of Defense (W81XWH-21-1-0789 to H.X. and X.H.-F.Z., DAMD W81XWH-16-1-0073, Era of Hope Scholarship to X.H.-F.Z.), the John S. Dunn Foundation Collaborative Research Award (to H.X.), and the Hamill Innovation Award (to H.X.). H.X. is a Cancer Prevention & Research Institute of Texas (CPRIT) scholar in cancer research.

■ REFERENCES

(1) Tran, L.; Xiao, J.-F.; Agarwal, N.; Duex, J. E.; Theodorescu, D. Advances in Bladder Cancer Biology and Therapy. *Nat. Rev. Cancer* **2021**, *21*, 104.
(2) Scott, A. M.; Wolchok, J. D.; Old, L. J. Antibody Therapy of Cancer. *Nat. Rev. Cancer* **2012**, *12* (4), 278−287.
(3) Marston, H. D.; Paules, C. I.; Fauci, A. S. Monoclonal Antibodies for Emerging Infectious Diseases — Borrowing from History. *N Engl J. Med.* **2018**, *378* (16), 1469−1472.
(4) Lu, L. L.; Suscovich, T. J.; Fortune, S. M.; Alter, G. Beyond Binding: Antibody Effector Functions in Infectious Diseases. *Nat. Rev. Immunol* **2018**, *18* (1), 46−61.
(5) Loupy, A.; Lefaucheur, C. Antibody-Mediated Rejection of Solid-Organ Allografts. *N Engl J. Med.* **2018**, *379* (12), 1150−1160.
(6) Trail, P.; Willner, D.; Lasch, S.; Henderson, A.; Hofstead, S.; Casazza, d A.; Firestone, R.; Hellstrom, I.; Hellstrom, K. Cure of Xenografted Human Carcinomas by BR96-Doxorubicin Immunoconjugates. *Science* **1993**, *261* (5118), 212−215.
(7) Perez, P.; Hoffman, R. W.; Shaw, S.; Bluestone, J. A.; Segal, D. M. Specific Targeting of Cytotoxic T Cells by Anti-T3 Linked to Anti-Target Cell Antibody. *Nature* **1985**, *316* (6026), 354−356.
(8) Carter, P.; Presta, L.; Gorman, C. M.; Ridgway, J. B.; Henner, D.; Wong, W. L.; Rowland, A. M.; Kotts, C.; Carver, M. E.; Shepard, H. M. Humanization of an Anti-P185HER2 Antibody for Human Cancer Therapy. *Proc. Natl. Acad. Sci. U. S. A.* **1992**, *89* (10), 4285−4289.
(9) Staerz, U. D.; Kanagawa, O.; Bevan, M. J. Hybrid Antibodies Can Target Sites for Attack by T Cells. *Nature* **1985**, *314* (6012), 628−631.
(10) Xiao, H.; Woods, E. C.; Vukojicic, P.; Bertozzi, C. R. Precision Glycocalyx Editing as a Strategy for Cancer Immunotherapy. *Proc. Natl. Acad. Sci. U. S. A.* **2016**, *113* (37), 10304−10309.
(11) Gray, M. A.; Stanczak, M. A.; Mantuano, N. R.; Xiao, H.; Pijnenborg, J. F. A.; Malaker, S. A.; Miller, C. L.; Weidenbacher, P. A.; Tanzo, J. T.; Ahn, G.; et al. Targeted Glycan Degradation Potentiates the Anticancer Immune Response in Vivo. *Nat. Chem. Biol.* **2020**, *16* (12), 1376−1384.
(12) Zhang, Y.; Wang, D.; Welzel, G.; Wang, Y.; Schultz, P. G.; Wang, F. An Antibody CDR3-Erythropoietin Fusion Protein. *ACS Chem. Biol.* **2013**, *8* (10), 2117−2121.
(13) Dai, Z.; Zhang, X.-N.; Nasertorabi, F.; Cheng, Q.; Li, J.; Katz, B. B.; Smbatyan, G.; Pei, H.; Louie, S. G.; Lenz, H.-J.; et al. Synthesis of Site-Specific Antibody-Drug Conjugates by ADP-Ribosyl Cyclases. *Sci. Adv.* **2020**, *6* (23), eaba6752.
(14) Cruz, E.; Kayser, V. Monoclonal Antibody Therapy of Solid Tumors: Clinical Limitations and Novel Strategies to Enhance Treatment Efficacy. *Biologics* **2019**, *13*, 33−51.
(15) Baker, J. H. E.; Kyle, A. H.; Reinsberg, S. A.; Moosvi, F.; Patrick, H. M.; Cran, J.; Saatchi, K.; Häfeli, U.; Minchinton, A. I. Heterogeneous Distribution of Trastuzumab in HER2-Positive Xenografts and Metastases: Role of the Tumor Microenvironment. *Clin Exp Metastasis* **2018**, *35* (7), 691−705.
(16) Pallasch, C. P.; Leskov, I.; Braun, C. J.; Vorholt, D.; Drake, A.; Soto-Feliciano, Y. M.; Bent, E. H.; Schwamb, J.; Iliopoulou, B.; Kutsch, N.; et al. Sensitizing Protective Tumor Microenvironments to Antibody-Mediated Therapy. *Cell* **2014**, *156* (3), 590−602.
(17) Kennecke, H.; Yerushalmi, R.; Woods, R.; Cheang, M. C. U.; Voduc, D.; Speers, C. H.; Nielsen, T. O.; Gelmon, K. Metastatic Behavior of Breast Cancer Subtypes. *J. Clin. Oncol.* **2010**, *28* (20), 3271−3277.
(18) Spadazzi, C.; Mercatali, L.; Esposito, M.; Wei, Y.; Liverani, C.; De Vita, A.; Miserocchi, G.; Carretta, E.; Zanoni, M.; Cocchi, C.; et al. Trefoil Factor-1 Upregulation in Estrogen-Receptor Positive Breast Cancer Correlates with an Increased Risk of Bone Metastasis. *Bone* **2021**, *144*, 115775.
(19) Riggio, A. I.; Varley, K. E.; Welm, A. L. The Lingering Mysteries of Metastatic Recurrence in Breast Cancer. *Br. J. Cancer* **2021**, *124* (1), 13−26.
(20) Gullo, G.; Zuradelli, M.; Sclafani, F.; Santoro, A.; Crown, J. Durable Complete Response Following Chemotherapy and Trastuzumab for Metastatic HER2-Positive Breast Cancer. *Ann. Oncol.* **2012**, *23* (8), 2204−2205.
(21) Fujisawa, R.; Wada, Y.; Nodasaka, Y.; Kuboki, Y. Acidic Amino Acid-Rich Sequences as Binding Sites of Osteonectin to Hydroxyapatite Crystals. *Biochimica et Biophysica Acta (BBA) - Protein Structure and Molecular Enzymology* **1996**, *1292* (1), 53−60.
(22) Goldberg, H. A.; Warner, K. J.; Li, M. C.; Hunter, G. K. Binding of Bone Sialoprotein, Osteopontin and Synthetic Polypeptides to Hydroxyapatite. *Connect Tissue Res.* **2001**, *42* (1), 25−37.
(23) Zhang, G.; et al. A Delivery System Targeting Bone Formation Surfaces to Facilitate RNAi-Based Anabolic Therapy. *Nat. Med.* **2012**, *18* (2), 307.
(24) Zhang, Y.; Wei, L.; Miron, R. J.; Shi, B.; Bian, Z. Anabolic Bone Formation Via a Site-Specific Bone-Targeting Delivery System by Interfering With Semaphorin 4d Expression: SEMA-4D BONE TARGETING SYSTEM FOR BONE FORMATION. *J. Bone Miner Res.* **2015**, *30* (2), 286−296.
(25) Dang, L.; Liu, J.; Li, F.; Wang, L.; Li, D.; Guo, B.; He, X.; Jiang, F.; Liang, C.; Liu, B.; et al. Targeted Delivery Systems for Molecular Therapy in Skeletal Disorders. *IJMS* **2016**, *17* (3), 428.
(26) Kingsley, L. A.; Fournier, P. G. J.; Chirgwin, J. M.; Guise, T. A. Molecular Biology of Bone Metastasis. *Molecular Cancer Therapeutics* **2007**, *6* (10), 2609−2617.
(27) Ren, G.; Esposito, M.; Kang, Y. Bone Metastasis and the Metastatic Niche. *Journal of Molecular Medicine* **2015**, *93* (11), 1203−1212.
(28) Ell, B.; Kang, Y. SnapShot: Bone Metastasis. *Cell* **2012**, *151* (3), 690.
(29) Drake, P. M.; Albers, A. E.; Baker, J.; Banas, S.; Barfield, R. M.; Bhat, A. S.; de Hart, G. W.; Garofalo, A. W.; Holder, P.; Jones, L. C.; et al. Aldehyde Tag Coupled with HIPS Chemistry Enables the Production of ADCs Conjugated Site-Specifically to Different Antibody Regions with Distinct in Vivo Efficacy and PK Outcomes. *Bioconjugate Chem.* **2014**, *25* (7), 1331−1341.

(30) Kilany, L. A. A.; Gaber, A. A. S.; Aboulwafa, M. M.; Zedan, H. H. Trastuzumab Immunogenicity Development in Patients' Sera and in Laboratory Animals. *BMC Immunology* **2021**, *22* (1), 15.
(31) Li, M.; Li, H.; Gao, K.; Wang, M.; An, W.; Zhu, Y.; Ding, L.; Wang, L.; Gu, J.; Zuo, C.; Sun, L. A Simple and Cost-Effective Assay for Measuring Anti-Drug Antibody in Human Patients Treated with Adalimumab. *Journal of Immunological Methods* **2018**, *452*, 6−11.
(32) Wang, H.; Tian, L.; Liu, J.; Goldstein, A.; Bado, I.; Zhang, W.; Arenkiel, B. R.; Li, Z.; Yang, M.; Du, S.; et al. The Osteogenic Niche Is a Calcium Reservoir of Bone Micrometastases and Confers Unexpected Therapeutic Vulnerability. *Cancer Cell* **2018**, *34* (5), 823.
(33) Wang, H.; Yu, C.; Gao, X.; Welte, T.; Muscarella, A. M.; Tian, L.; Zhao, H.; Zhao, Z.; Du, S.; Tao, J.; et al. The Osteogenic Niche Promotes Early-Stage Bone Colonization of Disseminated Breast Cancer Cells. *Cancer Cell* **2015**, *27* (2), 193−210.
(34) Zhang, W.; Bado, I. L.; Hu, J.; Wan, Y.-W.; Wu, L.; Wang, H.; Gao, Y.; Jeong, H.-H.; Xu, Z.; Hao, X.; et al. The Bone Microenvironment Invigorates Metastatic Seeds for Further Dissemination. *Cell* **2021**, *184* (9), 2471.
(35) Yamazaki, C. M.; Yamaguchi, A.; Anami, Y.; Xiong, W.; Otani, Y.; Lee, J.; Ueno, N. T.; Zhang, N.; An, Z.; Tsuchikama, K. Antibody-Drug Conjugates with Dual Payloads for Combating Breast Tumor Heterogeneity and Drug Resistance. *Nat. Commun.* **2021**, *12* (1), 3528.
(36) Lambert, J. M.; Chari, R. V. J. Ado-Trastuzumab Emtansine (T-DM1): An Antibody−Drug Conjugate (ADC) for HER2-Positive Breast Cancer. *J. Med. Chem.* **2014**, *57* (16), 6949−6964.
(37) Narayan, P.; Osgood, C. L.; Singh, H.; Chiu, H.-J.; Ricks, T. K.; Chow, E. C.; Qiu, J.; Song, P.; Yu, J.; Namuswe, F. FDA Approval Summary: Fam-Trastuzumab Deruxtecan-Nxki for the Treatment of Unresectable or Metastatic HER2-Positive Breast Cancer. *Clin. Cancer Res.* **2021**, *27*, 4478.
(38) Modi, S.; Saura, C.; Yamashita, T.; Park, Y. H.; Kim, S.-B.; Tamura, K.; Andre, F.; Iwata, H.; Ito, Y.; Tsurutani, J.; et al. Trastuzumab Deruxtecan in Previously Treated HER2-Positive Breast Cancer. *N Engl J. Med.* **2020**, *382* (7), 610−621.
(39) Yu, C.; Tang, J.; Loredo, A.; Chen, Y.; Jung, S. Y.; Jain, A.; Gordon, A.; Xiao, H. Proximity-Induced Site-Specific Antibody Conjugation. *Bioconjugate Chem.* **2018**, *29* (11), 3522−3526.
(40) Cao, Y. J.; Yu, C.; Wu, K.-L.; Wang, X.; Liu, D.; Tian, Z.; Zhao, L.; Qi, X.; Loredo, A.; Chung, A.; et al. Synthesis of Precision Antibody Conjugates Using Proximity-Induced Chemistry. *Theranostics* **2021**, *11* (18), 9107−9117.
(41) Hansel, T. T.; Kropshofer, H.; Singer, T.; Mitchell, J. A.; George, A. J. T. The Safety and Side Effects of Monoclonal Antibodies. *Nat. Rev. Drug Discov* **2010**, *9* (4), 325−338.
(42) Marty, M.; Cognetti, F.; Maraninchi, D.; Snyder, R.; Mauriac, L.; Tubiana-Hulin, M.; Chan, S.; Grimes, D.; Antón, A.; Lluch, A.; et al. Randomized Phase II Trial of the Efficacy and Safety of Trastuzumab Combined with Docetaxel in Patients with Human Epidermal Growth Factor Receptor 2-Positive Metastatic Breast Cancer Administered as First-Line Treatment: The M77001 Study Group. *J. Clin. Oncol.* **2005**, *23* (19), 4265−4274.
(43) Valero, V.; Forbes, J.; Pegram, M. D.; Pienkowski, T.; Eiermann, W.; von Minckwitz, G.; Roche, H.; Martin, M.; Crown, J.; Mackey, J. R.; et al. Multicenter Phase III Randomized Trial Comparing Docetaxel and Trastuzumab with Docetaxel, Carboplatin, and Trastuzumab as First-Line Chemotherapy for Patients with HER2-Gene-Amplified Metastatic Breast Cancer (BCIRG 007 Study): Two Highly Active Therapeutic Regimens. *J. Clin. Oncol.* **2011**, *29* (2), 149−156.
(44) Nahta, R.; Yu, D.; Hung, M.-C.; Hortobagyi, G. N.; Esteva, F. J. Mechanisms of Disease: Understanding Resistance to HER2-Targeted Therapy in Human Breast Cancer. *Nat. Clin Pract Oncol* **2006**, *3* (5), 269−280.
(45) Schmid, P.; Adams, S.; Rugo, H. S.; Schneeweiss, A.; Barrios, C. H.; Iwata, H.; Diéras, V.; Hegg, R.; Im, S.-A.; Shaw Wright, G.; et al. Atezolizumab and Nab-Paclitaxel in Advanced Triple-Negative Breast Cancer. *N Engl J. Med.* **2018**, *379* (22), 2108−2121.
(46) Tian, Z.; Wu, L.; Yu, C.; Chen, Y.; Xu, Z.; Bado, I.; Loredo, A.; Wang, L.; Wang, H.; Wu, K.; et al. Harnessing the Power of Antibodies to Fight Bone Metastasis. *Science Advances* **2021**, *7* (26), eabf2051.

https://doi.org/10.1021/acscentsci.1c01024
ACS Cent. Sci. 2022, 8, 312−321